A Review of Thrust Bearings Used in Rotary Air Preheaters

Bruce Fabijonas
Kingsbury, Inc. Philadel phia, Pennsylvania 19154

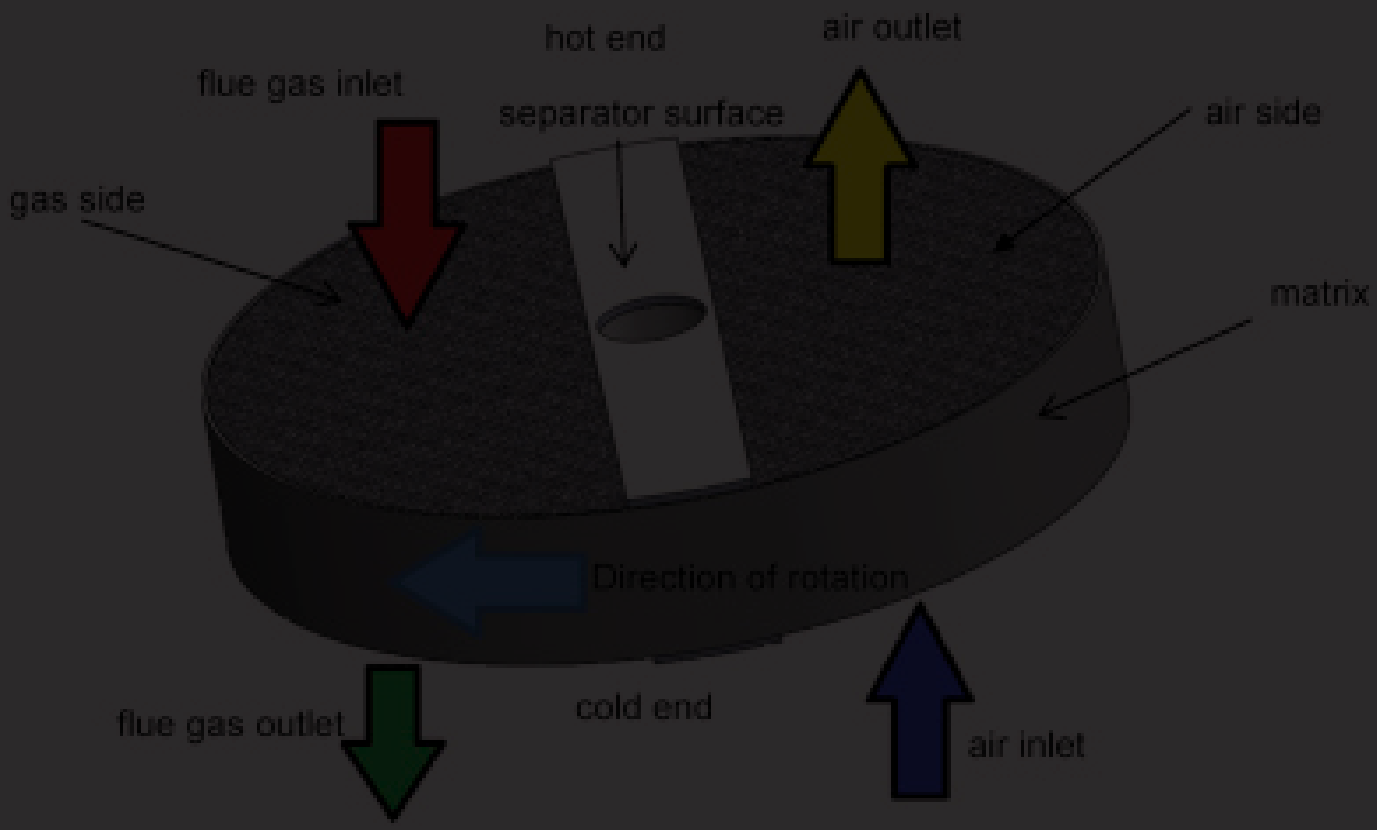

Kingsbury, Inc.®
Over 100 Years of Bearing Innovation

A review of thrust bearings used in rotary air preheaters
Revue de synthèse sur les butées hydrodynamiques utilisées dans les préchauffeurs à air rotatifs

Fabijonas BR [a]

a Kingsbury, Inc, 10385 Drummond Rd, Philadelphia, PA, 19154, USA.

Keywords: Thrust bearings, slow-speed/high-load, air pre-heaters, mixed-lubrication.
Mots clés : Butées hydrodynamiques, vitesse lente et charge élevée, les préchauffeurs à air rotatifs, lubrification mixte.

Rotary air pre-heaters are devices installed typically in power plants which reuse the heat of the exhaust gasses to heat the incoming fresh air, thus improving the plants' efficiency. The bearings used in these devices range from 580 mm to 2.2 m in diameter and are subjected to continuous loads in excess of 4 MPa at incredibly slow speeds, less than 0.1 m/s at mean diameter. Calculated minimum film thicknesses using a high-viscosity oil (1000 SSU at operating temperature) are on the order of 6 μm or smaller. Such conditions place the bearing in the mixed-lubrication region on a Stribeck curve. Nonetheless, Kingsbury has a long history of these bearings running successfully. We will review this history, discuss performance calculations, and speak to attempts to improve the bearings' operations.

Les préchauffeurs à air rotatifs sont des dispositifs installés généralement dans les centrales électriques qui réutilisent la chaleur des gaz d'échappement pour chauffer l'air frais entrant, améliorant ainsi l'efficacité des centrales. Les butées hydrodynamiques utilisées dans ces dispositifs ont un diamètre variant de 580 mm à 2,2 m et sont soumises à une pression spécifique permanente supérieure à 4 MPa et opérant à des vitesses incroyablement lentes, inférieures à 0,1 m/s au diamètre moyen. Les épaisseurs minimales calculées en utilisant une huile à haute viscosité (1000 SSU à la température de fonctionnement) sont de l'ordre de 6 μm ou voire inférieures. De telles conditions imposent la butée de fonctionner dans la zone de lubrification mixte sur une courbe de Stribeck. Néanmoins, Kingsbury a une longue histoire de bon fonctionnement de ces butées hydrodynamiques. Nous passerons en revue cet historique, discuterons des calculs de performance et parlerons des tentatives d'amélioration du fonctionnement des butées hydrodynamiques.

1 Introduction

1.1 Air Preheaters

An air preheater is a device that warms the fresh supply of air into a combustion chamber by transferring the heat in the exhaust gasses to the fresh air. It is a common component of coal-fired power generation plants. The most famous type of air preheater is the rotary regenerative type invented by Ljungström in 1920 and first commercially installed in 1922 [1]. The invention was so instrumental to the power generation industry that in 1995 it was declared an International Historic Mechanical Engineering Landmark by the American Society of Mechanical Engineers [2]. These machines rotate at exceptionally slow speeds. This paper discusses the use of fluid-film thrust bearings in these devices.

The basic design of a rotary regenerative air preheater (RRAP) is shown in Figure 1. Hot gases exit the combustion chamber (red arrow) and pass through a rotating drum of vertically aligned plates. As the drum slowly rotates, heat is transferred from the exit gasses to the plates. On the other side of the separator surface (in white), cool fresh air (blue arrow) passes through the now heated plates in the drum, and heat is transferred to the incoming air. The result is that the air entering the combustion chamber (yellow arrow) has risen in temperature far above the outside ambient. This process reduces the plant's power loss by not wasting energy raising the temperature of the incoming fresh air. The savings can be quite remarkable. In one example, exhaust gasses enter the device at 370°C and exit at 125°C; simultaneously, inlet air enters at 30°C and exits at 340°C [4]. It is estimated that for every 20°C drop in the flue gas temperature the fuel efficiency of the steam generator goes up by about 1% [5]. To facilitate the heat transfer, the rotating drum of transfer plates must rotate slowly. Typical speeds range around 1 rpm.

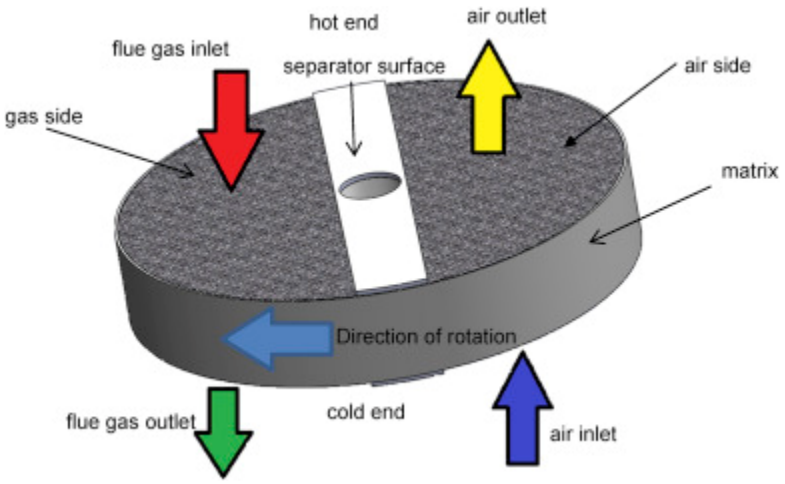

Fig 1 – Basic design of a Ljungstrom air preheater. From Ref. [3].

These machines are arranged vertically, and the thrust bearings typically sit in an enclosed oil bath either above or below the drum. The diameter of the bath is just slightly larger than the outer diameter of the shoes. Furthermore, no cooling mechanism for the oil exists. In fact, it is not uncommon for end-users to not install a thermocouple sensor to monitor the health of the bearing, something unthinkable in most applications of fluid-film bearings.

1.2 History of Thrust Bearings for Air Preheaters at Kingsbury

Small to modest size RRAPs use rolling element bearings. However, like their predecessors used in hydroelectric plants in the early 20th century, rolling element bearings fail to compete with the performance and life span of their fluid-film counterparts as the bearings increase in size.

In April 1948, Kingsbury Machine Works (now Kingsbury, Inc.) was approached to design a bearing to operate at 1 rpm for a 300K lbf (1.3 MN) load. A 23 in (584 mm) bearing was recommended at a cost of $1100. The competition was a rolling element bearing rated at 404K lbf (1.8 MN) load with 100,000 hour life span at a cost of $970. The price was critical because the customer was in stiff competition with tubular preheaters for the application. Kingsbury and its customer won each respective bid, and by November the bearing was installed and operational. The operator complained about "a slight grunt or chatter" when the machine started up, but once it was running, the bearing operated seamlessly. In August of 1952, the machine was taken offline for routine inspection. The bearing was found to be in perfect condition. Thus was the humble beginning of Kingsbury's line of air preheater bearings.

Since then, RRAP bearings have been a regular offering at Kingsbury, Inc. Over the years, many such bearings have been made, and some of our competitors entered the market as well. High pressure lift systems (HPLs) were introduced to help with startup chatter and assembly, though such systems come with their own set of headaches (described below).

1.3 Bearing Sizes and Ratings

Figure 2 graphically displays the current sizes and load ratings offered by Kingsbury. The values are based on Kingsbury's experience with these bearings and on the common sizes requested by our customers. The ratings assume an operating collar speed of 1 rpm and an oil satisfying a "1000 SSU at operating temperature" criterion. Here, "SSU" refers the Saybolt Second Universal measure of viscosity, also known as Saybolt Universal Seconds or "SUS." This criterion intentionally circumvents an oil selection due in part to the fact that the operating temperature is unknown. Indeed, very little heat generation in the oil is expected given the slow speed of the collar. Consequently, the operating temperature is a mix of various environmental temperatures (temperatures of the inlet and/or outlet gasses, degree of mixing within the oil pot, etc). The goal of this figure is to emphasize the high rated loads, especially for bearings with a high-pressure lift (HPL) mechanism, for shaft collars moving at 1 rpm.

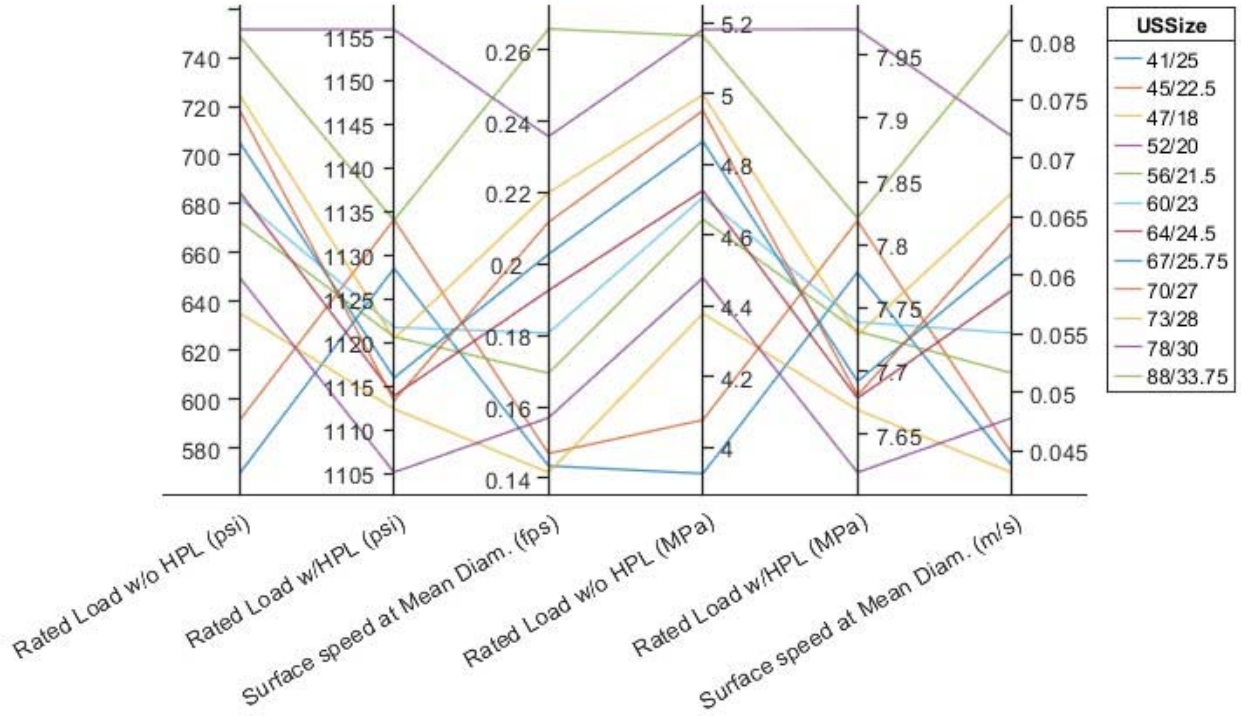

Fig 2 – Rated loads and surface speeds for the line of RRAP bearings at Kingsbury, Inc. Note how much higher the rated loads are for those with high pressure lift systems (HPLs).

1.4 Stribeck Curves

Every discussion about friction in tribology eventually refers to a Stribeck curve, a cartoon of which is drawn in Figure 3. Such a curve describes the change in the coefficient of friction as a function of the dimensionless Hersey number, defined as

$$H = \mu(T) \cdot \frac{V}{L}, \tag{1}$$

where μ is the dynamic viscosity in units of Pa-s at some temperature T, V is the velocity of the collar in units of m/s, and L is the is the applied load per unit length [6]. The Stribeck curve defines three regions by the curve's slopes—the boundary lubrication, the mixed lubrication, and the fully hydrodynamic regions. The physics of contact mechanics dominates the first region, the physics of fluid dynamics dominates the third, and a blend of the two types of physics dominates the mixed lubrication region.

Most Stribeck curves are generated experimentally, in part because the physics in all the regimes is not well modeled [7]. In such experiments, the dynamic viscosity and load are held constant, and the curves are generated as functions of velocity. Generating a Stribeck curve numerically remains a current avenue of research today. Indeed, any computer code intended to simulate a Stribeck curve would need to know the boundaries of the regions *a priori* to selectively choose which equations need to be solved.

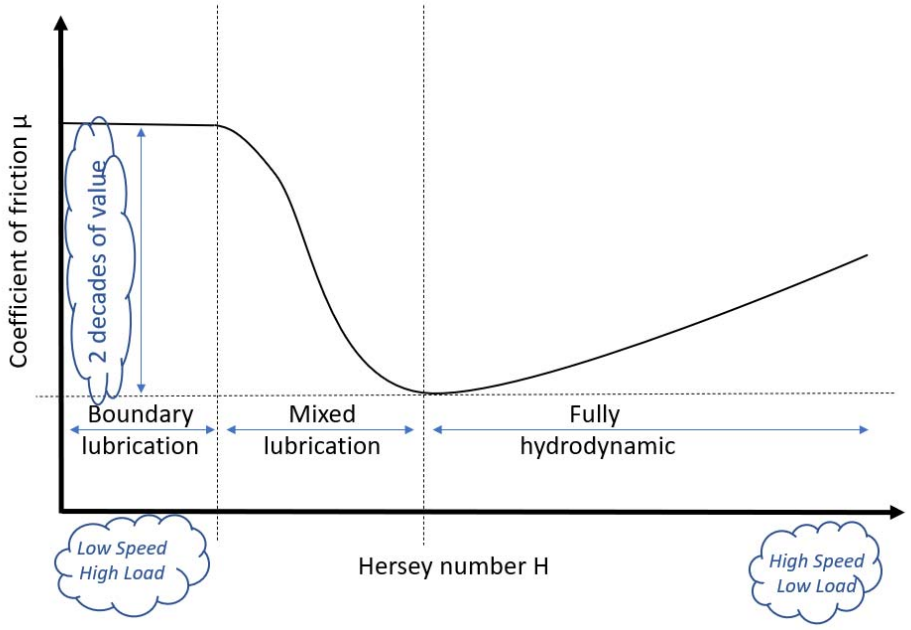

Fig 3 – Sketch of a typical Stribeck curve as a function of Hersey number.

The issue with using the Hersey number is that there is no universal set of values which separate the three operating regimes. From Eq. (1), one might be tempted to assume that a low-speed/high-load application like RRAP bearings should fall somewhere in the first two regions. Without concrete values on the abscissa in Figure 3, however, it is difficult to quantify where these bearings lie on the curve.

Alternatively, a more tangible parameter to describe the regions in a Stribeck curve is λ defined as the ratio of the minimum film thickness h_{min} to the root mean square of the roughness R_q of the two sliding surfaces:

$$\lambda = \frac{h_{min}}{R_q}, \qquad R_q = \sqrt{R_{q,runner}^2 + R_{q,shoe}^2}. \tag{2}$$

Almost all sources agree that border between the boundary and mixed lubrication regions occurs at $\lambda \approx 1$; the border between mixed and fully hydrodynamic regions typically lie near $\lambda \approx 3$ [8, 9, 10] though some high values like $\lambda \approx 10$ have been reported [11, 12]. We subscribe to the lower value.

2 Performance Calculations

The bearing that we will consider in this section has six shoes. Each shoe sweeps an angle of 51° with a 78 in (1981 mm) OD and a 30 in (762 mm) ID. The bearing is subjected to a 2.0 million pound (8.9 MN) load and is rotating at 1 rpm. The equations of oil viscosity are given in Table 1 and the corresponding constants in Table 2.

Equations for calculating dynamic viscosity as function of temperature	
T, T'	Temperature in K and °F, respectively
$A, T_0, API, a, b, c, \alpha, \beta, \gamma, \delta$	Constants listed in Table 2
$\nu(T) = \exp(\exp(A \ln(T/T_0))) - 0.7$	Mathieu model for kinematic viscosity in centistokes (cSt) as function of temperature T
$\sigma_{60} = 141.5/(API + 131.5)$	Specific gravity of oil at 60°F
$\sigma = \sigma_{60} * \left(a + bT' + cT'^2\right)$	σ is the specific gravity of an oil at temperature T'
$\rho_w = \alpha + \beta T' + \gamma T'^2 + \delta T'^3$	Density of water in units of g/cm^3
$\mu(T') = \sigma(T')\rho_w(T')\nu(T')$,	Dynamic viscosity in centipoise (cP)
$cSt = 0.22 * (SSU) - 180/(SSU)$	Conversion between Saybolt Second Universal and cSt.

Tab 1 – Equations for the temperature dependence of oil.

ISO VG	API	A	T_0	Coefficient	Value
32	29.3	-3.66608	436.9470	a	1.02423
46	28.7	-3.84635	441.5476	b	-4.08863×10^{-4}
68	27	-3.67412	460.7024	c	8.00713×10^{-8}
100	27.1	-3.72743	466.9379	α	0.997526898
150	25.7	-3.59577	485.5313	β	0.000141952
220	25.7	-3.42646	508.5245	γ	-2.12817×10^{-6}
320	25.7	-3.40836	520.7926	δ	2.80861×10^{-9}
460	25.7	-3.33684	539.0068		
680	25.7	-3.16156	566.0569		

Tab 2- Constants used in the equations in Tab 1.

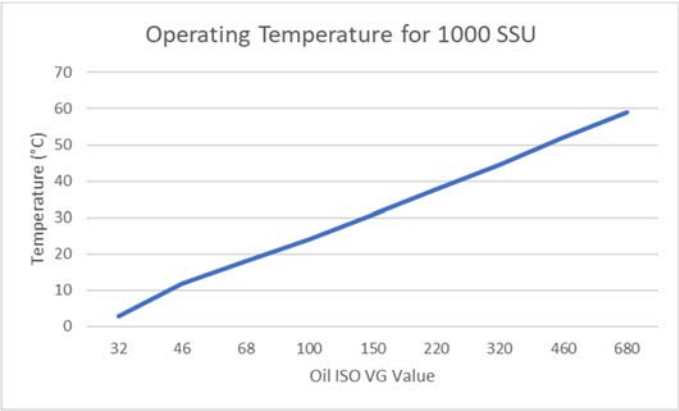

Fig 4– Operating temperatures for different oil grades that correspond to 1000 SSU.

2.1 Hand Calculations of the 1950s

The original performance calculations of the 1950s contained a minimum film thickness calculation derived from the Reynolds equation for an infinite wedge slider bearing with a constant linear profile and a side-leakage factor [13, 14]. The minimum film thickness was calculated using an equation similar to

$$h_o = \sqrt{\frac{6\mu u \ell K_p L}{P_{ave}}} \,. \tag{3}$$

Here, μ is the fluid dynamic viscosity of the oil at a given temperature, u is the surface speed of the collar at mean diameter, ℓ is the circumferential length of a thrust shoe, L is a dimensionless side leakage factor, P_{ave} is the film pressure averaged by the area of the loaded bearing surface, and K_p is an integration constant. Values for K_p and side leakage factor can be found in Ref. [14].

The "1000 SSU at operating temperature" criterion mentioned above corresponds to a minimum film thickness value of 0.5 mils (12.3 μm) using Equation 3. One can only conclude that the engineers of the 1950s must have felt that that this was an acceptable lower bound for minimum film thickness for the bearing under consideration. We can relate this criterion to a Stribeck curve as follows: assuming a 32 Ra finish (in microinches) on the collar and the thrust shoe, the criterion corresponds to $\lambda = 10.6$ and thus lies in the fully hydrodynamic region. From Table 1, the value of 1000 SSU corresponds to kinematic viscosity of 219.8 cSt. Using Mathieu's model for viscosity and the constants in Table 2, we generate a graph of ideal operating temperatures as a function of oil viscosity grade in Figure 4. Operating temperatures above the curve correspond to lower SSU values (less viscous, which in turn means smaller film thicknesses), and those below the curve correspond higher SSU values (more viscous and larger film thicknesses).

The solid lines in Figure 5 are plots of the calculated minimum film thickness using Equation 3 as for different viscosity grades and operating temperatures. Figure 5 also includes a plot of the calculated minimum film thickness for the "1000 SSU at operating temperature" criterion. Anything below this last curve fails to meet the criterion for successful operation. Figure 5 demonstrates that the low viscosity grade oils yield minimum film thicknesses well below the 0.5 mils limit. Indeed, the film thickness calculations indicate that using an oil as viscous as ISO VG 680 will push the application into the fully hydrodynamic region for a large range of temperatures.

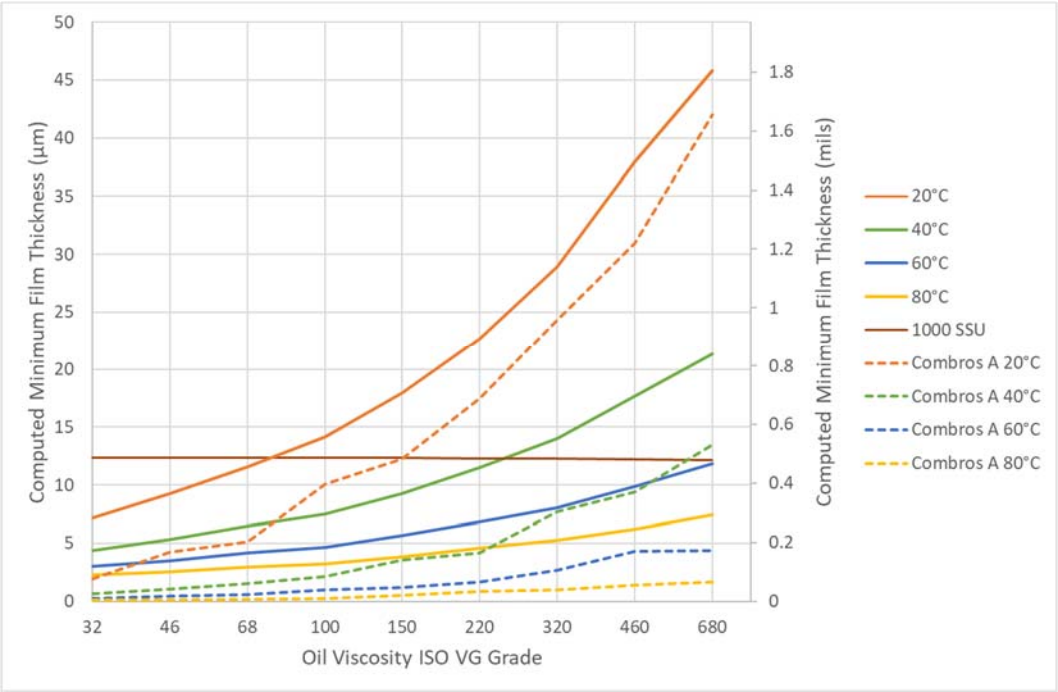

Fig 5 – Minimum film thickness predictions using Equation 3 (solid lines) and extrapolation of data generated by Combros A (dashed lines). Included are the film thickness calculations for different viscosity grades at "1000 SSU at operating temperature."

2.2 Typical Bearing Performance Model

Bearings for RRAPs are a challenge for modern performance prediction codes. We present results generated by the three-dimensional thermo-elasto-hydrodynamic code COMBROS-A [15]. It comes as no surprise that direct computation of an extremely high load rotating at 1 rpm is almost impossible. To simplify convergence, we set the code to isothermal conditions. We saw a negligible difference in the computed minimum film thickness when compared to a smattering of non-isothermal calculations. At moderate temperatures, the code can successfully compute cases up to 40% or 50% of the target load for high viscosity grades and 20%-30% for lower viscosity grades. This improves with lower operating temperatures up to 100% for ISO VG 680 at 20°C. Figure 6 shows the results of the calculations at 50°C. To generate data at full load, we extrapolate the minimum film thickness using a quadratic curve fit to the data in Fig. 5A on a log-log plot of film thickness vs load fraction to generate the dashed curves in Figure 5.

A comparison of the solid and dashed curves in Figure 5 is challenging. Since the data points on the dashed curves are extrapolations, they are to be taken with caution. Extrapolation inherently assigns a specific behavior to the physics in the problem that may or may not be valid. For example, pad deflection is inherently nonlinear and can dramatically change as loads increase from 20% to 100% of full-load. A change of pad deflection can significantly reduce the load-carrying area of the pad, which in turn changes all of the dynamics of the problem. Recall that Equation 3 does not take any kind of pad deflection into consideration. The conclusion that we can draw is that calculation of a minimum film thickness remains an open question for these bearings. Clearly, a detailed finite-element analysis of these bearings is in order, but that lies beyond the scope of this paper.

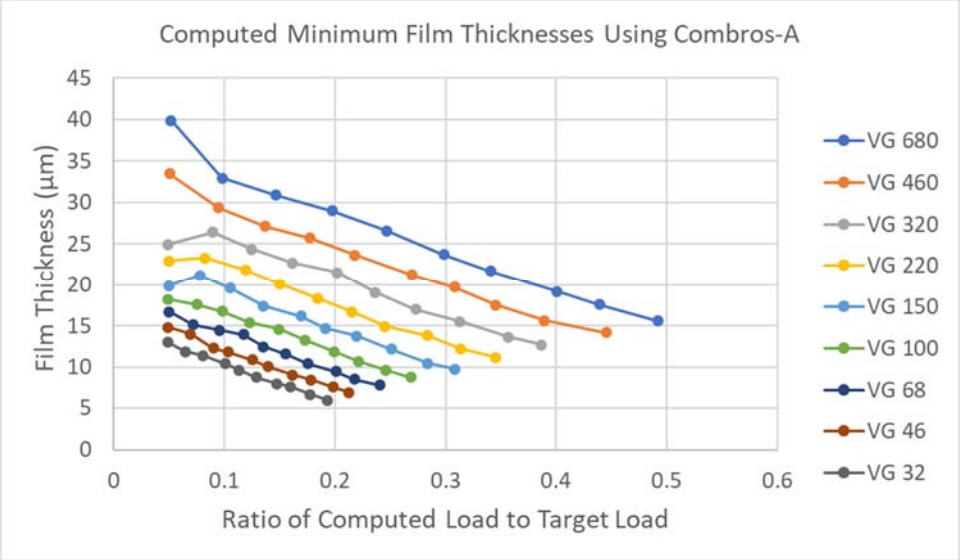

Fig 6– Computed minimum film thicknesses for a range of loads at 1 rpm and 50°C using Combros-A with isothermal conditions. Computation of the minimum film thicknesses in Figure 6 come from extrapolation of this and similar data.

3 Field Challenges

We list a few of the challenges with RRAP bearings encountered by Kingsbury staff over the years.

- The biggest challenge that hinders these bearings from running successfully is the environment in which they operate. As can be imagined, coal-burning power plants are not the most sterile of environments. One particular nuisance is that these plants have airborne ash particles at all times. Should the seals on the bearing housing fail, the ash contaminates the oil in the housing. The ash embeds itself in the babbitt of the thrust bearing shoes and effectively acts like coarse-grit sandpaper against the runner. In trying to clean up the shoes when this happens, the affected shoes often damage cutting tools when attempting to perform a skim-cut of the bearing surface to remove the ash particles.
- RRAPs which operate in cold environments far from the equator can experience temperatures in which ISO VG 680 oil appears to be frozen. Add to this the possibility that the operating temperature of the bearing can be significantly different between the two halves of the RRAP (the gas side and the air side—see Figure 1), and the problem can become complicated quickly.
- Compounding the environment challenge is the bearing design. Typically, the base ring is machined into the RRAP housing by the vendor, and the bearing manufacturer merely supplies the leveling plates and the shoes. This means that the bearing is assembled on site by power plant mechanics rather than turbomachinery specialists.
- The assembly method of the RRAPs takes a heavy toll on the bearings. The heat transfer drum of the RRAP is assembled in pie-shaped sections after the bearing is in place. These sections are hard to maneuver and are inserted one section at a time 180° apart through an access panel with little clearance. The rotor is spun using chains and come-alongs hard against the almost dry face of the thrust bearing for the next pie-shaped section.
- Although HPL systems can help the above-mentioned assembly process, they come with their own set of headaches:
    - their cost is prohibitive in a marketplace with thin margins;
    - the tight fit between the OD of the shoe and the base ring necessitates that the supply lines for the HPL be attached at either the leading or trailing edges without hindering the motion of the shoes;
    - the extreme temperatures involved in the problem could wreak havoc on the temperature distribution within the oil film when oil is injected through the supply hole, or "freeze" can occur within the HPL system itself;

- and the lack of a reservoir from which the HPL could pull and/or exit add levels of complexity to the problem.

4 Conclusions

We have presented a brief history of RRAP bearings at Kingsbury, Inc. Although these bearings intuitively lie in the boundary lubrication portion a Stribeck curve, they remain in the fully hydrodynamic region with the proper choice of oil. We demonstrate the challenges in predicting bearing performance numerically. And finally, we discuss how their operating environments are not conducive to successful operation. Yet in the face of these challenges, the fluid-film thrust bearings for RRAPs perform well at speed of 1 rpm, and sometimes even less.

5 Acknowledgements

The author thanks his colleagues Fred Wiesinger and Matt Marchione at Kingsbury, Inc. for their input on this paper including personal recollections from various projects. The author is indebted to his late mentor Scan DeCamillo who had compiled a history of these bearings within Kingsbury.

6 References

[1] Warren I. (1982) Lundström heat exchangers for waste heat recovery. Journal of Heat Recovery Systems, 2(3), 257-271.

[2] AMSE Historic Landmark #185: Ljungstrom Air Preheater (1920). https://www.asme.org/about-asme/engineering-history/landmarks/185-ljungstrom-air-preheater.

[3] Heidari-Kaydan A. & Hajidavalloo E. (2014) Three-dimensional simulation of rotary air preheater in steam power plant. Applied Thermal Engineering, 73, 399-407.

[4] The Howden Group Limited, Rotary Heater Technology, http://www.howden.com.

[5] Hariharan Power Private Limited, http://hariharanpower.com/airpreheater.php.

[6] Khonsari MM & Booser ER. (2010) On the Stribeck curve. In GK Nikas (Ed) Recent Developments in Wear Prevention, Friction, and Lubrication, pp. 263-278.

[7] Zhang Y, Biboulet N, Venner CH & Lubrecht AA. (2020) Prediction of the Stribeck curve under full-film elastohydrodynamic lubrication. Trib. Int. 149, 105569.

[8] Wäsche R & Woydt M. (2014) Stribeck Curve. In T Mang (Eds) Encyclopedia of Lubricants and Lubrication, pp. 1998-2005, Springer. https://doi.org/10.1007/978-3-642-22647-2_274.

[9] Shirzadegan M. (2016) Elastohydrodynamic Lubrication of Cam and Roller Follower Applications: Fast and Reliable Predictions of Friction. PhD Thesis, Luleå University of Technology.

[10] Ramirez MA & Pritchard R. (2020) A novel solid lubricant uses the principles of tribology to reduce the coefficient of friction (COF) in oil-based muds (OBM) for extended reach drilling applications. Society of Petroleum Engineers, SPE-199033-MS, 26pp.

[11] Nicholas G, Clarke BP & Dwyer-Joyce RS. (2021) Detection of lubrication state in a field operational wind turbine gearbox using ultrasonic reflectometry. Lubricants, 9(6), 23pp.

[12] Hamel M, Addali A & Mba D. (2014) Monitoring oil film regimes with acoustic emission. Proc IMechE Part J: J Eng Trib, 228(2), 223-231.

[13] Fuller DD. (1956) Theory and Practice of Lubrication for Engineers. New York: John Wiley & Sons.

[14] DeCamillo SM & Fabijonas BR (2012) Chapter 45: Thrust Bearings. In RW Bruce (Ed) Handbook of Lubrication and Technology, Vol 2, 21pp., CRC Press. https://doi.org/10.1201/b12265.

[15] Kraft, C (2023) User Manual Thrust Bearing Calculation Program COMBROS-A v2.0, ITR, TU Clausthal: Clausthal, Germany.

[16] Fabijonas BF & Rodzwic RC (2021) A Comparative Study of Flooded and Directed-Lubrication Fluid-Film Thrust Bearings at High Load and Speed Conditions. Proceedings of the 51st Turbomachinery Symposium, Turbomachinery Laboratory, Texas A&M Engineering Experiment Station; Texas A&M University Libraries, 22pp.